OXIDE INDUCED FATIGUE CRACK CLOSURE AND NEAR-THRESHOLD CHARACTERISTICS IN A508-3 STEEL

Hideo Kobayashi, Takeshi Ogawa, Haruo Nakamura and Hajime Nakazawa
Tokyo Institute of Technology, Japan

INTRODUCTION

In stage II, plane-strain, linear elastic fracture mechanics fatigue crack growth, growth rates, da/dN, under constant amplitude loading have been well related to stress intensity factor ranges, $\Delta K = K_{max} - K_{min}$, where K_{max} and K_{min} are maximum and minimum stress intensity factors, respectively. At intermediate ΔK values (stage IIb, striation mechanism), this relation takes a simple power law [1]

$$da/dN = C\ \Delta K^m \qquad (1)$$

where m and C are supposed to be material constants. A double-logarithmic plot of da/dN versus ΔK would then be a straight line, as shown in Fig. 1. Crack growth characteristics in stage IIb are insensitive to microstructure, environment and the stress ratio, $R = K_{min}/K_{max}$, and have been explained on the basis of plasticity induced crack closure [2, 3]. At low ΔK values (stage IIa), however, da/dN deviates from Eq. (1) and decreases abruptly to a vanishingly small value. Conceivably there is a threshold value of ΔK, namely ΔK_{th}, below which no crack growth occurs at all, as shown in Fig. 1. Near-threshold characteristics are very sensitive to microstructure, environment and R and have been explained on the basis of fretting oxide induced crack closure [4, 5] or fracture surface roughness induced crack closure [6]. Questions still remain, however, with respect to the specific influence of the above-mentioned factors.

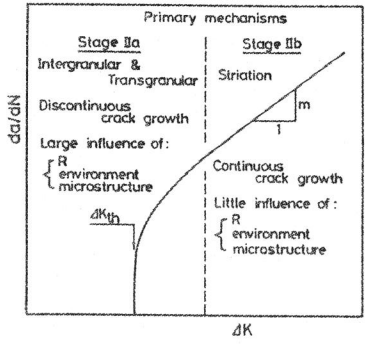

Fig. 1 Fatigue crack growth characteristics.

The object of the present study is to develop an improved understanding of near-threshold characteristics through further consideration of crack closure and the influence of R.

MATERIAL AND EXPERIMENTAL PROCEDURE

The material used was an A508-3 steel (yield strength: 465 MPa, tensile strength: 595 MPa). Specimens used were of the ASTM compact type with W = 51.0 mm and B = 12.5 mm. The crack path was in the L-T orientation. The specimens were tested on a MTS feedback-controlled testing machine using load as the control parameter. Two types of tests, R-constant tests (R = 0.06, 0.3 and 0.7) and K_{max}-constant tests (K_{max} = 10.8, 15.5 and 31.0 MPa$\sqrt{m}$), were conducted in an air environment at room temperature. Crack lengths were determined using a travelling microscope. In general, all of the testing and data analysis procedures for ASTM E647 [7] and an ASTM E24.04 working document [8] were adhered to. Crack closure was monitored by an ultrasonic method. A 5 mm diameter, 10 MHz compression probe was used to monitor the specularly reflected signal from a growing fatigue crack during each load cycle.

RESULTS

Figure 2 shows relations between da/dN and ΔK in the R-constant tests. For the cases that R = 0.06 and 0.3, da/dN decreases abruptly as ΔK decreases from Eq. (1) below 5×10^{-9} m/cycle. Fretting oxide debris exist on the fracture surfaces corresponding to these regions, as shown in Fig. 3, which may suggest that oxide induced crack closure has an important role on near-threshold characteristics for these cases. For the case that R = 0.7, Eq. (1)

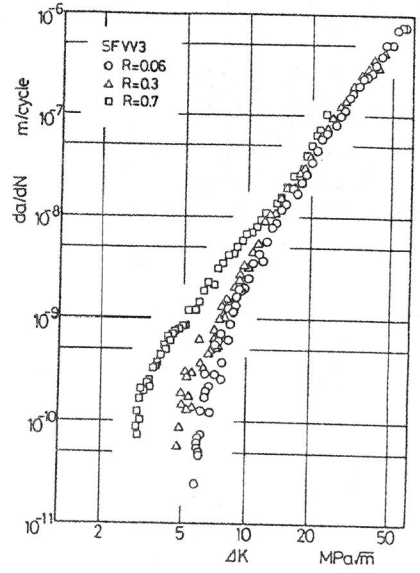

Fig. 2 Relations between da/dN and ΔK in R-constant tests.

stands above 10^{-10} m/cycle and the fretting oxide debris do not exist on the fracture surface, except a narrow zone corresponding to ΔK_{th}.

Figure 4 shows relations between K_{op}/K_{max} and K_{max}, where K_{op} is an opening level of the stress intensity factor. When $K_{op} < K_{min}$, unloading was attempted to evaluate apparent K_{op} values which are denoted by solid symbols in Fig. 4. The values of K_{op}/K_{max} due to plasticity induced crack closure become nearly constant regardless of K_{max} for a given R value, except low K_{max} regions where K_{op}/K_{max} sweeps upward as K_{max} approaches threshold conditions due to oxide induced crack closure.

Figure 5 shows relations between da/dN and ΔK_{eff}, where ΔK_{eff} are effective stress intensity factor ranges ($\Delta K_{eff} = K_{max} - K_{op}$ for $K_{op} > K_{min}$ and $\Delta K_{eff} = K_{max} - K_{min}$ for $K_{op} < K_{min}$). The relations become a following equation regardless of R

$$da/dN = C'\Delta K_{eff}^{2} \qquad (2)$$

where C' is a material constant.

The above-mentioned R-constant, ΔK-decreasing tests involve the stepping down of K_{max} and K_{min} for a given R value. On the other hand, the K_{max}-constant, ΔK-decreasing tests involve the stepping up of K_{min}

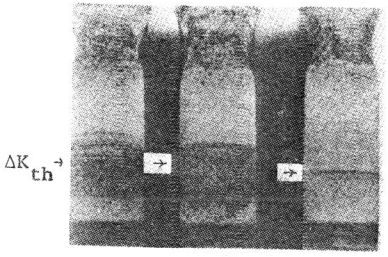

Fig. 3 Fracture surfaces.

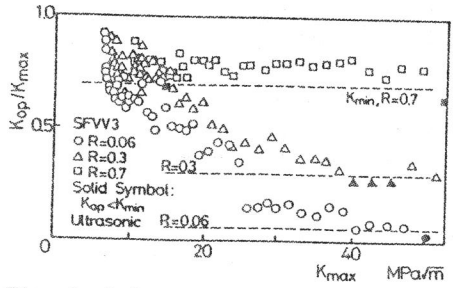

Fig. 4 Relations between K_{op}/K_{max} and K_{max} in R-constant tests.

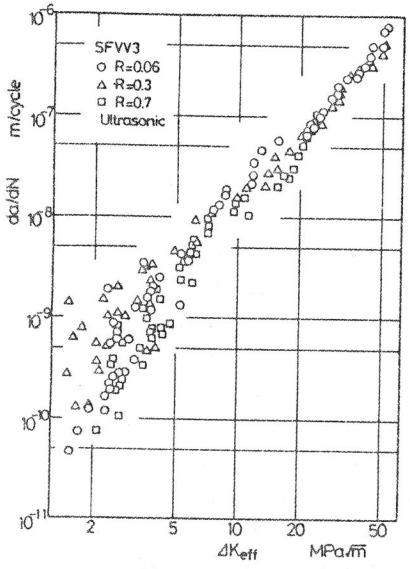

Fig. 5 Relations between da/dN and ΔK_{eff} in R-constant tests.

for a given K_{max} value.

Figure 6 shows relations between da/dN and ΔK in the K_{max}-constant tests. The da/dN-ΔK curves for R = 0.06, 0.3 and 0.7 in the R-constant tests are also shown in Fig. 6. For the case that K_{max} = 10.8 MPa$\sqrt{m}$, da/dN decreases gradually as ΔK decreases following the da/dN-ΔK curves corresponding to each R value. Observation of the fracture surface shows that oxide induced crack closure has an important role in this case, as shown in Fig. 7. On the other hand, for the cases that K_{max} = 15.5 and 31.0 MPa$\sqrt{m}$, Eq. (1) stands above 10^{-10} m/cycle and relations between da/dN and ΔK are in excellent agreement with that for R = 0.7 except ΔK_{th}, regardless of K_{max}, although the values of R varies from 0.3 to 0.8 (K_{max} = 15.5 MPa$\sqrt{m}$) or from 0.5 to 0.9 (K_{max} = 31.0 MPa$\sqrt{m}$) as ΔK decreases. In these cases, the fretting oxide debris do not exist on the fracture surface at all.

That is to say, if a contribution of oxide induced crack closure is excluded, the near-threshold characteristics become insensitive to R and plasticity induced crack closure alone has an important role on them. The value of non-oxide controlled ΔK_{th}, determined at $da/dN = 10^{-10}$ m/cycle, becomes 2.7 MPa$\sqrt{m}$ regardless of R in this steel. It should be

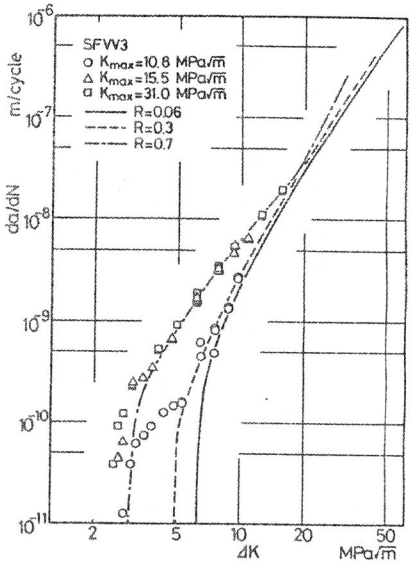

Fig. 6 Relations between da/dN and ΔK in K_{max}-constant tests.

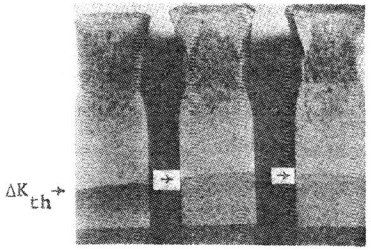

Fig. 7 Fracture surfaces.

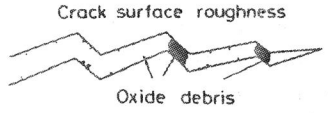

Fig. 8 Schematic diagram showing crack surface roughness and fretting oxide debris.

noted that a slightly higher value of ΔK_{th} for R = 0.7 is attributed to a little contribution of oxide induced crack closure as stated earlier.

After the R-constant, ΔK-decreasing tests, the specimens were sectioned and observation was carried out by a scanning electron microscope. In the near-threshold region, transgranular and intergranular shear modes of crack growth are dominant and the crack contour is rough, as shown in Fig. 8 schematically, which may promote partial contact of crack surfaces [6]. As a result, the fretting oxide debris are produced not uniformly but partially between the crack surfaces. That is to say, the fracture surface roughness may be a trigger for production of the fretting oxide debris. So, both have a close relation each other.

DISCUSSIONS

Figure 9 shows relations between ΔK_{th} and R, where the values of oxide controlled and non-oxide controlled ΔK_{th} were obtained in the R-constant tests and the K_{max}-constant tests, respectively. The crack growth characteristics not only at intermediate ΔK values but also of near-threshold become insensitive to R, if the contribution of oxide induced crack closure is excluded (see Fig. 6). Likewise, the values of non-oxide controlled ΔK_{th} would become insensitive to R. Figure 9 also includes such data estimated from the da/dN-ΔK relations for K_{max} = 15.5 and 31.0 MPa$\sqrt{m}$ in the K_{max}-constant tests. In these cases, the characteristics are controlled only by plasticity induced crack closure. So, differences between oxide controlled and estimated ΔK_{th} for a given R value show quantitatively the contribution of oxide induced crack closure. The contribution becomes remarkable as R decreases. In the case that the crack growth characteristics at intermediate ΔK values are insensitive to microstructure and environment as well as R, the values of non-oxide controlled ΔK_{th} would also become a structure- and environment-insensitive material constant (see Fig. 9).

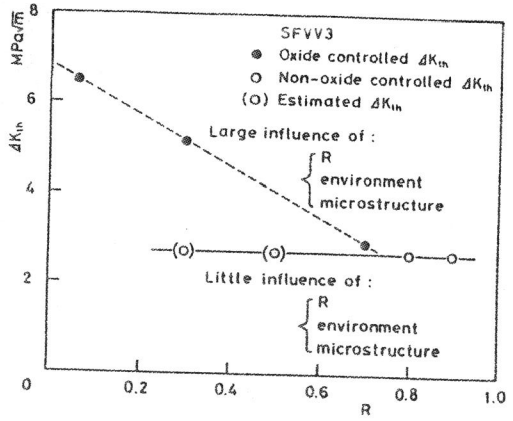

Fig. 9 Relations between ΔK_{th} and R in R- and K_{max}-constant tests.

CONCLUSION

The near-threshold characteristics in fatigue crack growth for the A508-3 steel were investigated. The results obtained are summarized as follows:

(1) Fretting oxide induced crack closure has an important role on the near-threshold characteristics obtained by the R-constant, ΔK-decreasing tests.

(2) It can be possible to exclude the contribution of oxide induced crack closure on the near-threshold characteristics by the K_{max}-constant, ΔK-decreasing tests. In this case, the characteristics are controlled only by plasticity induced crack closure.

(3) The values of non-oxide controlled ΔK_{th} become a material constant regardless of R in this steel.

REFERENCES

[1] Paris, P.C. and Erdogan, F., A Critical Analysis of Crack Propagation Laws, Trans. ASME, Ser. D, Journal of Basic Engineering, 85 (1963), 528/534.

[2] Elber, W., The Significance of Fatigue Crack Closure, Damage Tolerance in Aircraft Structure, ASTM STP 486, 230/242 (1971).

[3] Kobayashi, H., Nakamura, H. and Nakazawa, H., Mechanics of Fatigue Crack Growth: Comparison between Fatigue and Ideal Cracks, Mechanics of Fatigue, AMD - Vol. 47, ASME, 133/150 (1981).

[4] Stewart, A.T., The Influence of Environment and Stress Ratio on Fatigue Crack Growth at Near-Threshold Stress Intensities in Low-Alloy Steels, Engineering Fracture Mechanics, 13 (1980), 463/478.

[5] Suresh, S., Zamiski, G.F. and Ritchie, R.O., Oxide-Induced Crack Closure: An Explanation for Near-Threshold Corrosion Fatigue Crack Growth Behaviour, Metallurg. Trans., 12A (1981), 1435/1443.

[6] Minakawa, K. and McEvily, A.J., On Crack Closure in the Near-Threshold Region, Scripta Metallurgica, 15 (1981), 633/636.

[7] ASTM Standard Test Method for Constant-Load-Amplitude Fatigue Crack Growth Rates above 10^{-8} m/cycle (E647-81), Annual Book of ASTM Standards, Part 10, 765/783 (1981).

[8] Proposed ASTM Test Method for Measurement of Fatigue Crack Growth Rates, Fatigue Crack Growth Mesurement and Data Analysis, ASTM STP 738, 340/356 (1981).